Available online at www.sciencedirect.com
SCIENCE DIRECT®
International Journal of Heat and Mass Transfer 48 (2005) 4562–4568
International Journal of HEAT and MASS TRANSFER
www.elsevier.com/locate/ijhmt

Detection of hot spot through inverse thermal analysis in superconducting RF cavities

A. Aizaz [a,*], R.L. McMasters [b]

[a] National Super Conducting Cyclotron Laboratory (NSCL), South Shaw Lane, MSU, East Lansing, MI 48824, United States
[b] Department of Mechanical Engineering, MSU East Lansing, MI 48824, United States

Received 16 August 2004; received in revised form 28 February 2005

Abstract

An inverse heat conduction problem in a superconducting radio frequency (SRF) cavity is examined. A localized defect is simulated as a point-heating source on the inner surface (RF surface) of the evacuated niobium cavity. Liquid helium acts as a coolant on the outer surface of the cavity. By measuring the outer surface temperature profile of the cavity using relatively few sensors, the temperature and location of a hot spot on the inner surface of the niobium are calculated using an inverse heat conduction technique. The inverse method requires a direct solution of a three-dimensional heat conduction problem through the cavity wall thickness along with temperature measurements from sensors on the outer surface of the cavity, which is immersed in liquid helium. A non-linear parameter estimation program then estimates the unknown location and temperature rise of the hot spot inside the cavity. The validation of the technique has been done through an experiment conducted on a niobium sample at room temperature.

Keywords: SRF cavity; Inverse heat transfer; Thermal sensor; Heat conduction

1. Introduction

A key component of the modern particle accelerator is the device that imparts energy to the charged particles. This is the electromagnetic cavity resonating at a microwave frequency at very low temperatures where the material of the cavity is electrically superconducting. Thermal breakdown, or quench, is a phenomenon where the temperature of part or all of the entire RF surface of the cavity exceeds the critical temperature T_c, thereby becoming non-superconducting, rapidly dissipating all stored energy in the cavity fields. Temperature mapping of the outer surface of the cavity thus becomes an essential tool in the diagnostics of the performance degradation of the cavity. In practice, usually the temperature mapping of the outer surface is accomplished using several hundred arbitrarily spaced sensors to identify the local hot spot on the RF surface. Due to the very high sensitivity of the carbon sensors at 1.6 K, detection of a temperature rise of 60 μK above ambient has been reported by Padamsee et al. [1]. However, quantitative estimation of actual temperature rise on the hot spot has not been made in previous research. It is the purpose of this research to quantitatively estimate not only the location, but also the actual temperature rise of the hot spot on the RF surface. In this paper, we shall first present the mathematical model employed in the

* Corresponding author. Tel.: +1 517 333 6317.
E-mail address: aizazahm@msu.edu (A. Aizaz).

0017-9310/$ - see front matter © 2005 Elsevier Ltd. All rights reserved.
doi:10.1016/j.ijheatmasstransfer.2005.05.034

three-dimensional numerical technique. This is done by performing a steady state analysis to determine the minimum number of temperature sensors, with suitable spacing, required at a specific bath temperature to detect a temperature rise of 60 μK above ambient. The numerical data thus obtained shall provide sufficient information to aid in employing an inverse heat conduction technique to make estimates of the unknown parameters, namely the location of the hot spot and the associated temperature rise on the RF surface. Comparing the results of this program with the exact solution provides code verification. Later in this paper, the information obtained from the numerical experiment, along with experimental data, provides not only the desired unknown parameters, but also the validation for the code.

2. Numerical simulations

2.1. Model definition

The region of interest for the SRF 805 MHz cavity is modeled as a rectangular parallelepiped 3-D surface, as shown in Fig. 1. This section of the cavity is chosen to be a representative region. A more detailed view of this three-dimensional surface with sensors installed on the outer (cooled) surface, is shown in Fig. 2. The sensors are encased in an insulated housing to protect against the direct cooling effects of liquid helium. The details of the construction of the housing are given elsewhere [1,2].

2.2. Governing differential equation

From a typical order of magnitude analysis, the transient time constant, known as Fourier number $\left(Fo = \frac{\alpha' t}{L_c^2}\right)$, is quite large for niobium cavities even for small times of several milliseconds (e.g. *Fo* for 1 mm thick Nb at 50 ms time interval is 775), and steady state conditions are reached very rapidly. In this relation, α' is the thermal diffusivity of the niobium in $\left(\frac{\text{cm}^2}{\text{s}}\right)$, L_c, is the thickness of the niobium in (cm) and, t is time in (s).

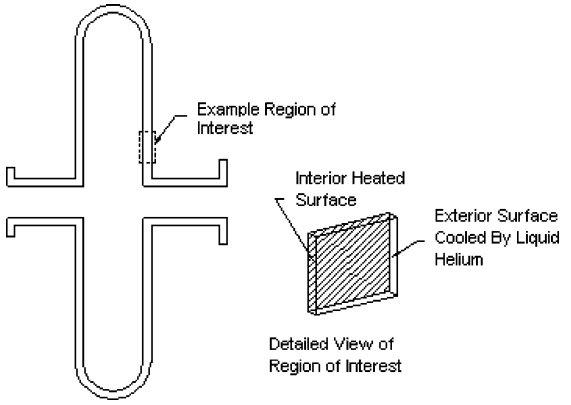

Fig. 1. Region of interest (ROI) on an elliptical superconducting 805 MHz cavity is modeled as a rectangular parallelepiped surface with point heat source on the interior surface and cooled by the liquid helium on the exterior surface.

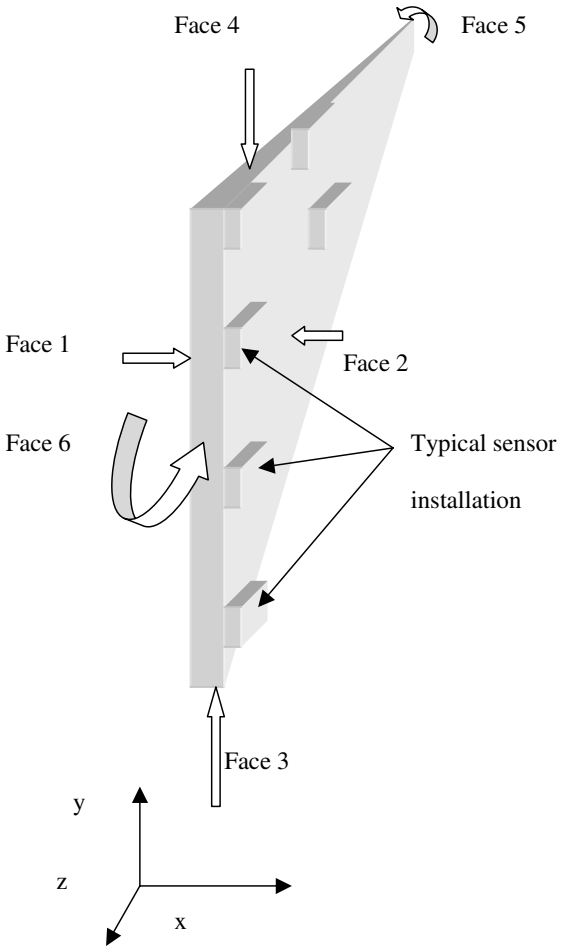

Fig. 2. The rectangular parallelepiped surface of ROI has a heat source on face 1 and the sensors on face 2 are shown placed arbitrarily where liquid helium cools to the desired operating temperature. The *x*-axis is chosen in the direction along the thickness of the niobium metal.

For this steady state condition, in the absence of any source of internal heat generation inside the cavity material, the heat transport equation in the cavity is described by

$$\frac{\partial^2 T}{\partial x^2} + \frac{\partial^2 T}{\partial y^2} + \frac{\partial^2 T}{\partial z^2} = 0 \tag{1}$$

2.3. Boundary conditions

The boundary conditions on each of the six faces are described with respect to the faces identified in Fig. 2.

On face 1, zero heat flux ($q|_{yz(\text{except Pt.heat})} = 0$) is imposed except on the point of heating. At the point of heating, user input is required to specify the heat flux. Face 2 also has two different kinds of boundary conditions, depending upon the location of sensors. The surface on face 2 exposed to liquid helium has a convective boundary condition, similar to the one described later. However, the surface on face 2 exposed to the sensor is given by

$$q|_{\text{Nb}} = q|_{\text{Sensor}}$$
$$T_{\text{Nb(interface)}} = T_{\text{Sensor(interface)}}$$

Though the insulated sensor housing is made of several materials, the G-10 used in the casing of the sensor (an epoxy filled fiber glass commonly used in the cryogenic industry) is assumed to have thermal properties close to those of the epoxy and the carbon sensor. All other faces, i.e., 3, 4 and 5, 6 are modeled as adiabatic boundaries. On the sensor itself, a convective boundary condition, as given below, is valid for the remaining five sides of the housing.

$$q|_{\text{sensor}} = h|_{\text{conv,He}}\Delta T$$

Here, $h_{\text{conv,He}}$ is the kapitza conductance of liquid helium when it is below its lambda transition temperature, i.e., below 2.17 K. Though this quantity is highly temperature dependent, for the purpose of small temperature differences (on the order of milli Kelvin), its value is assumed to be constant and mainly dependent upon the bulk liquid helium temperature. However, for experiments above the lambda transition temperatures, i.e., $T_{\text{He}} > 2.17$ K, liquid helium for the purpose of heat transfer can be considered as an ordinary fluid [6]. The value of $h_{\text{conv,He}}$ then depends upon the state of the pool boiling liquid.

Although many commercial programs are available to solve the Laplace equation, they do not provide the degree of flexibility required for generating solutions which could be used in an iterative scheme for nonlinear parameter estimation. Therefore, a custom-made code is developed as part of this research that could serve as a program subroutine in the overall parameter estimation program.

2.4. Discretization of the differential equation

The discretization of the differential equation is done using a second order central finite difference technique. This discretized equation can be solved through the successive over relaxation (SOR) iterative technique. The final form of the equation is given as

$$T^{n+1}_{i,j,k} = T^{n}_{i,j,k} + \omega\left[\frac{1}{\lambda}\{\alpha(T^{n+1}_{i-1,j,k} + T^{n}_{i+1,j,k}) + \beta(T^{n+1}_{i,j-1,k} + T^{n}_{i,j+1,k}) + \gamma(T^{n+1}_{i,j,k-1} + T^{n}_{i,j,k+1})\} - T^{n}_{i,j,k}\right] \quad (2)$$

Here, the superscript "$n+1$" is the current iteration number, "n" is the previously computed iteration number and, $\gamma = \Delta y^2\Delta x^2$, $\alpha = \Delta y^2\Delta z^2$, $\beta = \Delta z^2\Delta x^2$, $\lambda = 2(\Delta x^2\Delta y^2 + \Delta x^2\Delta z^2 + \Delta z^2\Delta y^2)$. "$\omega$" is the convergence acceleration parameter which varies between 1 and 2 and is determined through numerical experimentation. Similarly, the boundary equations are developed from discretization of the boundary conditions using the finite control volume approach. One example of the algebraic equations developed for the boundary conditions is taken from the interface boundary between the niobium surface and the casing of the sensor housing, as shown in Fig. 2.

$$T^{n+1}_{i,j,k} = \frac{1}{\lambda}\left[\alpha\left\{\left(\frac{2K_{\text{Nb}}}{K_{\text{Nb}} + K_{\text{G-10}}}\right)T^{n+1}_{i-1,j,k} + \left(\frac{2K_{\text{G-10}}}{K_{\text{Nb}} + K_{\text{G-10}}}\right)T^{n}_{i+1,j,k}\right\} + \beta(T^{n+1}_{i,j-1,k} + T^{n}_{i,j+1,k}) + \gamma(T^{n+1}_{i,j,k-1} + T^{n}_{i,j,k+1})\right] \quad (3)$$

Here, K_{Nb} is the thermal conductivity of niobium; $K_{\text{G-10}}$ is the thermal conductivity of the G-10. Also, 'i', 'j', and 'k' are the usual indices for x, y, and z directions, respectively.

2.5. Convergence

Since the numerical formulation of the 'Laplace' equation, along with its boundary equations through the SOR technique gives a positive definite matrix, convergence is readily ensured [3]. Grid refinement on the code is done to a level that ensures the final form of the solution is grid independent. The convergence criteria are satisfied when less than a 0.1% change in all parameter values is observed between iterations.

2.6. Numerical results and post-processing

As shown in Fig. 3, the highest temperature locations on the cooled surface are the four corners where sensors are installed because of the insulating effects of the sensors. The heater simulates as a hot spot in this configuration, symmetrically centered on face 1 in the 'yz' plane (see Fig. 2). Due to the relatively high thermal conductivity of niobium at low temperatures, heat generated by a point source is conducted away within the metal and a very low temperature rise is expected at the outer surface of the cavity. Moreover, the rise in temperature on the cooled surface to be detected by the sensors is greatly influenced by the excellent cooling properties of super fluid helium.

Fig. 4 shows the relationship between the sensor efficiency and the sensor spacing for different thicknesses of the niobium plate. Sensor efficiency here is defined as the ratio of temperature rise on the cooled surface to the

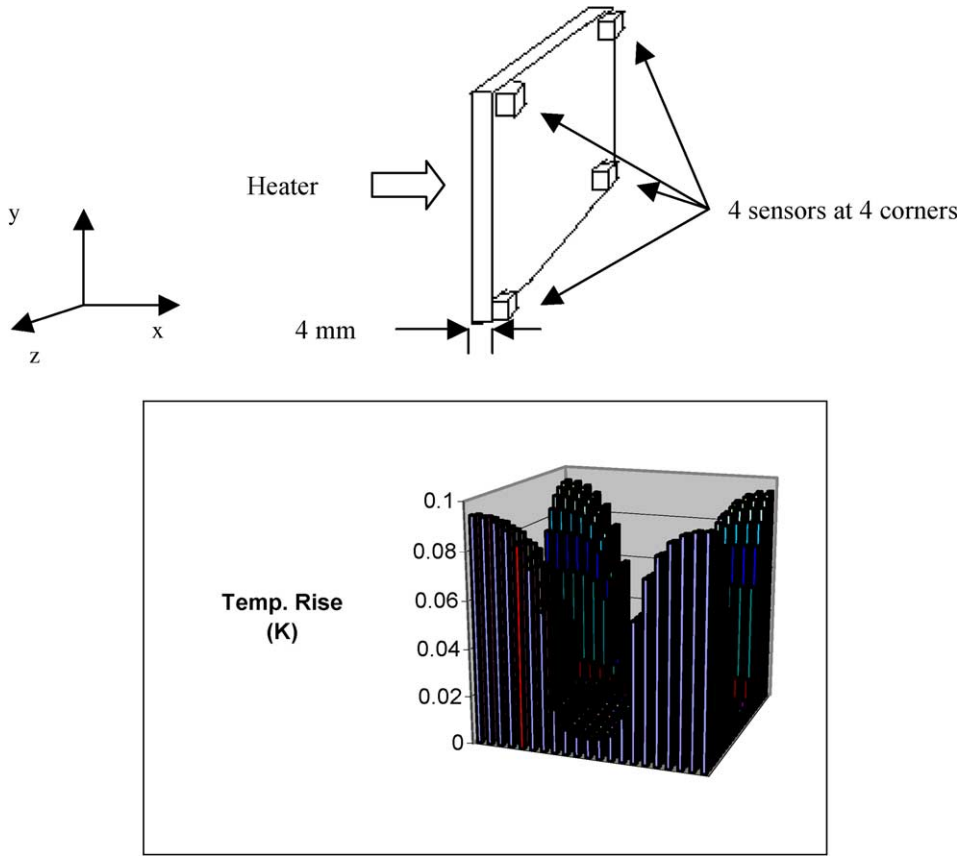

Fig. 3. Program output showing the highest temperature locations at the four corners of the outer (cooled) surface on '*yz*' plane. Four sensors are located at the four corners on the cooled surface and the heater is symmetrically located in the center of the RF surface. Thickness of the plate is 4 mm.

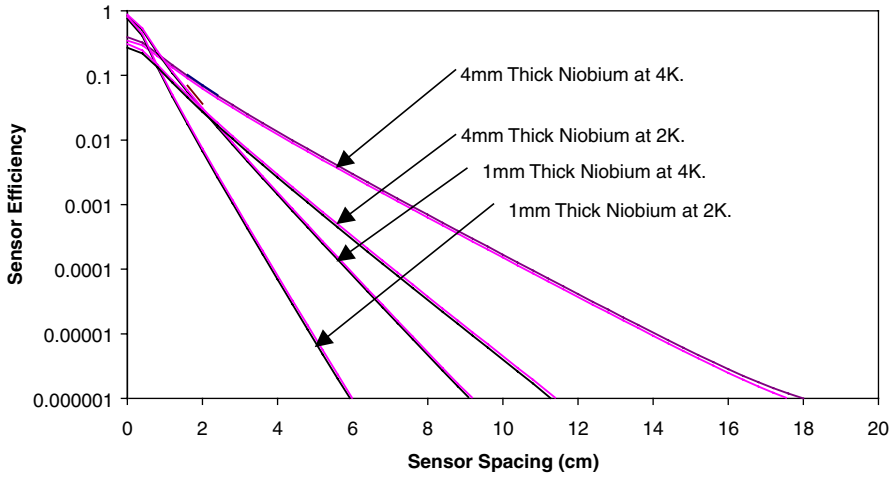

Fig. 4. Sensor efficiency as a function of sensor spacing for various temperatures and niobium thicknesses. Three solutions included at each condition: CON3D (bare plate), the Code (insulated sensors), and FEM solution.

maximum temperature rise of the hot spot on the RF surface. Since the sensor efficiency is a function of the distance between the sensors (sensor spacing), the sensor efficiency calculations are repeated for each thickness of

niobium plate, i.e., 1 mm and 4 mm, and for each value of selected bulk temperature of liquid helium, i.e., 2 K and 4 K. Code verification is done with the results obtained through the exact solutions generated by COND3D [4] without sensors and through the Kokopelli Finite Element Method program [5]. As shown in Fig. 4, the results obtained from all three computer programs are in good agreement with each other, with maximum errors of 1% or less, and this only at very small sensor spacings. From these plots, the effect of the presence of the sensors on the final solution of the problem is seen to be nearly negligible. This is mainly attributable to the relatively small sensor size (1 cm × 0.4 cm × 0.3 cm) as compared with the overall dimensions of the plate in the problem, which are on the order of tens of centimeters.

3. Program validation

The validity of the model is shown by comparing the results obtained from the program with the experimental data. Since the magnitude and location of a heating source in an operational cavity cannot be experimentally verified, an experiment was performed at room temperature with a known heat source to validate the method. Six thermocouples as shown in Fig. 5, were used to record the temperature of the cold surface of a 4 mm thick niobium plate.

A thin foil heater of 1.27 cm diameter with negligibly small thickness (on the order of micrometer) is used to act as the 2-D source of heating for the model problem. The bottom surface, i.e., the heated surface, is then insulated using sheets of G-10 material. An insulating tape is used to bond the plate and the sheets together which also provides insulation to the side walls of the niobium plate to match the boundary condition as closely to those of the model as possible. The error induced due to possible heat leaks to the insulated G-10 and the boundaries is estimated to be less than 3%. Also, the possible heat leaks through the heater and sensor wires are estimated to be less than 1% of the total heat input. The experimental data obtained is then compared with the data obtained from the program. As shown in Fig. 6, the two results, i.e., from the experiment and the one computed are in agreement with each other. As shown in Table 1, the standard deviation of the difference between the two is 0.045 K.

4. Inverse heat conduction calculations

To estimate the location as well as temperature of the hot spot on the RF surface of the cavity, the inverse heat conduction technique through non-linear parameter estimation is employed. Here, the three desired parameters are the unknown temperature at the heated niobium surface and the 'y' and 'z' coordinates of the heater.

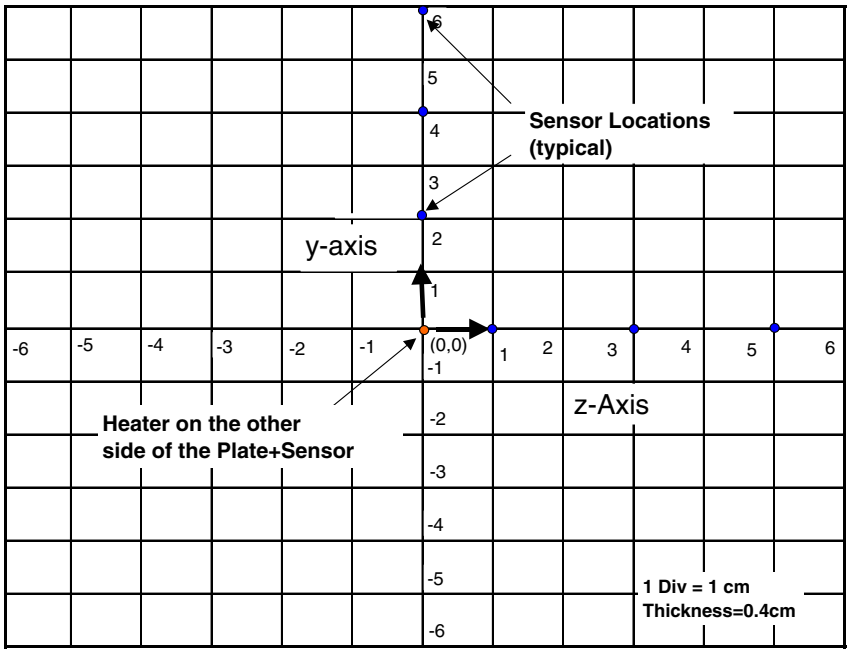

Fig. 5. Experimental setup to validate the computational model. Six sensors placed 1 cm apart over a 4 mm thick niobium plate with heater and a sensor installed on the bottom surface.

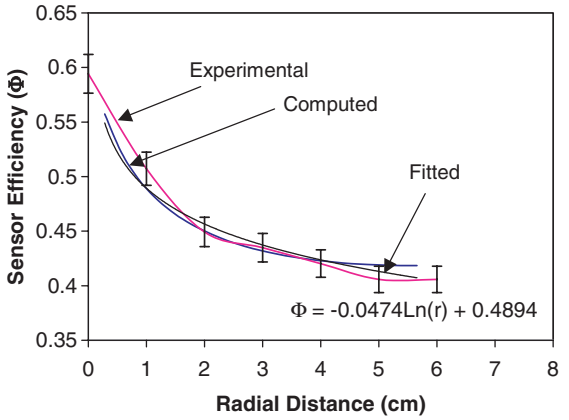

Fig. 6. Sensor efficiency (Φ) shown as a function of radial distance (r). The relationship obtained from numerical computation is compared with the one obtained from the experimental setup at room temperature.

From the definition of sensor efficiency, we know that

$$\Phi(r) = T(r)_i / T_{\max} \tag{4}$$

where $\Phi(r)$ is the sensor efficiency and is a function of distance 'r' given as

$$r = \sqrt{(y - y_i)^2 + (z - z_i)^2} \tag{5}$$

Here, (y,z) is the unknown location of the heat source and (y_i, z_i) is the known location of the sensor 'i' with respect to a rectangular grid system arbitrarily set over the plate, $T(r)_i$, is the temperature rise at a distance 'r' measured by the sensor 'i', and $T_{\max}$ is the unknown maximum temperature rise on the heated surface of the plate, i.e., the temperature rise of the heater. In matrix form this equation can be written as

$$[T_i] = T_{\max}[\Phi(r_i)] \tag{6}$$

In this equation, as described above, $T_{\max}$, and the coordinates (y,z) of the heater (which determines the value of r_i) are the only unknowns. Now if we have six temperature sensors installed on the top (cold) surface of the plate to detect the heat produced by the heater on the bottom (hot) surface of the plate, then each sensor shall have an efficiency curve as a function of its location 'r_i' away from the point of heating. Such a curve for each sensor is obtained from iteratively using the direct computation of the 3-D steady state program described above, and using the fact that location of each sensor is also known. Thus from the above procedure, we shall have the following six equations, one for each sensor.

$$T_1 = T_{\max}\Phi(r_1)$$
$$T_2 = T_{\max}\Phi(r_2)$$
$$\vdots$$
$$T_6 = T_{\max}\Phi(r_6)$$

In this set of six equations, we have just three unknowns. So we have an over-defined set of equations whose unique solution does not exist. The unknown values (y, z and $T_{\max}$) can be obtained using the functional form of $\Phi(r_i)$ as the direct solution. The three unknown parameters are then found by minimizing the sum of squares of the errors between the measured temperature rise and the calculated temperature rise at each sensor location. The estimation method utilizes finite difference sensitivity coefficients with a step size of 0.1%. Specifically, the values of y, z, and $T_{\max}$ are found which minimize $S^2 = \sum_{i=1}^{6}(Y_i^2 - T_i^2)$ where Y_i represents the measured temperature rise and T_i represents the calculated temperature rise above ambient. The convergence criteria are satisfied when less than a 0.1% change in all parameter values is observed between iterations.

Table 1
The difference between the actual temperature rise and the estimated temperature rise at each sensor location by using inverse heat conduction technique

Verification of estimated parameters through inverse technique				
Z (cm)	Y (cm)	Measured temp rise (K)	Estimated temp rise (K)	Error
1	0	3.5	3.44	−0.06
0	2	3.1	3.11	0.01
3	0	3	3.04	0.04
0	4	2.9	2.89	.01
5	0	2.8	2.86	0.06
0	6	2.8	2.78	−0.02
			Std. dev (K)	0.045
		Parameter estimated		Experimental
Max temp rise (K)		6.90		6.9
Z (cm)		0.222		0
y (cm)		−0.278		0

The close agreement of the two results, as shown in Table 1, validates the use of the direct model and the inverse method. If the values of the estimated parameters are then used and substituted back to calculate the temperature rise detected by each sensor, the difference between the measured temperature rise from the sensor and the calculated temperature rise is quite small with a standard deviation of only 0.045 K.

5. Conclusion

An 805 MHz SRF cavity has been modeled to obtain the temperature map on the outer surface of the cavity. On post-processing of this mapped surface temperature data, a relationship has been obtained between sensor efficiency and the radial distance from the hot spot on the heated surface, for different wall thickness of niobium metal and for different bulk temperatures of liquid helium. This relationship determines the maximum sensor spacing allowed to detect a one-degree rise in the temperature on the RF (heated) surface to give a rise of 60-μK-on the cooled surface. The numerical model for this work has been validated by experimental measurements at room temperatures. The inverse heat conduction technique has been applied on the numerical as well as experimental data to obtain the unknown thermal parameters of the cavity.

Acknowledgements

The authors would like to thank T. Grimm and W. Hartung of the National Super Conducting Laboratory (NSCL) MSU for providing useful insight on SRF cavities. Thanks are also due to J. Colthorp and S. Hitchcock of NSCL for extending their help in accomplishing the experiment.

References

[1] H. Padamsee, J. Knobloch, T. Hays, RF Superconductivity for Accelerators, Wiley, New York, 1998, p. 166.
[2] J. Knobloch, Advanced thermometry studies of Superconducting RF cavities, PhD thesis, Cornell University, Ithaca, NY, 1997.
[3] B. Carnahan, J.O. Wilkes, Numerical methods optimization techniques and process simulation for engineers, 1967, p. 279.
[4] J. Beck, R.L. McMasters, A. Haji-Sheikh, Computer Code COND3D, Under Contact to Sandia National Laboratories, Albuquerque, NM, 2002.
[5] D. Tullock, E. Montalbano, Finite Element Program Kokopelli 96.2, Los Alamos National Laboratory, Los Alamos, NM, 1996.
[6] S.W. Van Sciver, Helium Cryogenics, Plenum, 1986.